JOURNAL OF THERMOPHYSICS AND HEAT TRANSFER
Vol. 17, No. 2, April–June 2003

Development of a Variable Emittance Radiator Based on a Perovskite Manganese Oxide

Sumitaka Tachikawa* and Akira Ohnishi†
Institute of Space and Astronautical Science, Kanagawa 229-8510, Japan
Yuichi Shimakawa‡ and Atsushi Ochi§
NEC Corporation, Tokyo 108-8001, Japan
and
Akira Okamoto¶ and Yasuyuki Nakamura**
NEC TOSHIBA Space Systems, Ltd., Kanagawa 224-8555, Japan

Two types of thermal control materials developed for space use are described. These new materials use a variable emittance radiator called the smart radiation device (SRD). The SRDs are based on $La_{0.825}Sr_{0.175}MnO_3$ and $La_{0.7}Ca_{0.3}MnO_3$ and comprise a thin and light ceramic tile. The materials undergo a metal–insulator transition near room temperature, and this allows the infrared emissivity of the device to change from low to high as the temperature is increased from 173 to 375 K. This is beneficial for thermal control applications on spacecraft. For example, bonded only to the external surface of the spacecraft, the SRD controls the heat radiated to deep space without electrical instruments or mechanical parts. Its function is similar to the thermal louver, but the SRD is lighter. This new device reduces the energy consumption of the electrical heater for thermal control and decreases the weight and the cost of the thermal control system. Optical properties, such as the total hemispherical emittance and the solar absorptance, have been measured. Space environmental simulation tests were performed with independent irradiation by protons, electrons, and UV on the ground. Degradation of the materials' optical properties is discussed.

Nomenclature

A	=	surface area, m^2
I_b	=	spectral distribution of emissive power of blackbody, $Wm^{-2}\mu m^{-1}$
I_s	=	solar extraterrestrial irradiance, $Wm^{-2}\mu m^{-1}$
Q	=	heater power, heat loss, W
R	=	reflectance
T	=	temperature, K
T_C	=	transition temperature, K
X	=	doping level
α_S	=	solar absorptance
ε_H	=	total hemispherical emittance
ε_{high}	=	total hemispherical emittance in high emittance state
ε_{low}	=	total hemispherical emittance in low emittance state
θ	=	angle of incidence, deg
λ	=	wavelength, m
σ	=	Stephan–Boltzmann constant, 5.67×10^{-8} $Wm^{-2}K^{-4}$

Subscripts

s	=	sample
w	=	wall, wire

Received 28 June 2002; revision received 16 October 2002; accepted for publication 16 October 2002.

*Research Engineer, Engineering Support Division, 3-1-1 Yoshinodai, Sagamihara. Member AIAA.
†Research Assistant, Center for Advanced Spacecraft Technology, 3-1-1 Yoshinodai, Sagamihara. Member AIAA.
‡Principal Researcher, Fundamental Research Laboratories, 5-7-1 Shiba, Minato.
§Principal Researcher, Functional Materials Research Laboratories, 5-7-1 Shiba Minato.
¶Manager, Mechanical Systems Department, 4035 Ikebe, Tsuzuki, Yokohama.
**Assistant Manager, Mechanical Systems Department, 4035 Ikebe, Tsuzuki, Yokohama.

Introduction

SPACECRAFT usually expel excess heat into deep space with radiators, keeping the temperature of all of the elements of a spacecraft system within the allowable limits for all mission phases. The amount of heat radiated into deep space is not constant because the temperatures of these elements are affected by heat inputs that are highly variable with time over the life of the mission. Thus, some devices are required for active thermal control. Traditionally, active thermal control is applied using heaters, variable conductance heat pipes, and mechanical louvers.[1] For small satellites, all of these approaches could require more mass or power than is available. A new, more flexible approach is a radiator coating with a variable infrared emissivity that can be actively adjusted in response to variations in the thermal load and environmental conditions. There have been several ideas for implementing such variable emissive surfaces, including microelectromechanical surfaces, electrochromic devices, and electrophoretic devices, as well as thermochromic devices.

We propose a variable emittance radiator that does not require any control instruments. It is a light ceramic tile that changes its emissivity according to its own temperature. Two types of the thermal control materials that we have developed are $La_{0.825}Sr_{0.175}MnO_3$ and $La_{0.7}Ca_{0.3}MnO_3$. Both are made of manganese oxides with a perovskite structure. The demands on the new thermal control device are 1) high optical performance for thermal control, 2) radiation durability, 3) low weight, and 4) no requirement for electrical power or mechanical parts.

This paper presents results summarizing experimental research on thermal control surfaces for spacecraft using a thermochromic device.

Smart Radiation Devices (SRDs)

Smart radiation devices (SRDs) are made of $La_{1-X}Sr_XMnO_3$ and $La_{1-X}Ca_XMnO_3$, which are manganese oxides with a perovskite

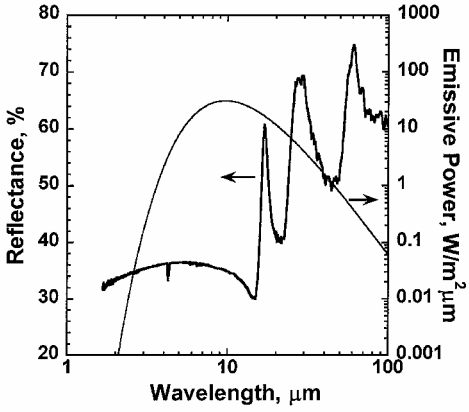

Fig. 1 Spectral reflectance of SRD at around ——, room temperature and blackbody radiation spectra at ——, 300 K.

structure. These are made by replacing La^{3+} with Sr^{2+} or Ca^{2+} in the parent material, $LaMnO_3$, which is an insulator. By this substitution, Mn^{3+} changes to Mn^{4+} to conserve electrical charge, and the material shows a phase change. The SRD is composed of mixed-valency manganite of perovskite structure, such as $(La_{1-X}Sr_X)(Mn^{3+}_{1-X}Mn^{4+}_X)O_3$, which exhibits a rich phase diagram.[2] For low doping levels under $X \approx 0.16$, the material changes its phase from a spin-canted antiferomagnetic insulator or a ferromagnetic insulator to a paramagnetic insulator with increasing temperature. On the other hand, for high doping levels over $X \approx 0.26$, the material changes its phase from a ferromagnetic metal to a paramagnetic metal with increasing temperature. For doping levels of $0.16 < X < 0.26$, the material changes its phase from a ferromagnetic metal to a paramagnetic insulator with increasing temperature. The resistivity of the material at this doping level changes between 10^{-3} and 10^{-1} Ωcm with temperature in the range between 173 and 373 K. The metallic state in these compounds is stabilized by the double-exchange interaction.[3] The transition temperature increases from around 150 to 350 K with the doping level. By selection of the optimum doping level, the material has the special property of being a metal–insulator transition at around room temperature. The material with the optimum molar ratio changes from metallic to a highly resistive state at the transition temperature; therefore, its reflectance changes drastically with the temperature.

Figure 1 shows the IR reflectance spectra of the SRD ($La_{0.825}Sr_{0.175}MnO_3$) at room temperature, obtained by a Fourier-transform infrared spectrometer (FT–IR), Bio-Rad FTS-60A/896, with a variable angle reflection accessory (The Seagull™; Harrick Science Corporation). Figure 1 also shows the blackbody radiation spectra at 300 K, which is determined by Planck's spectral distribution of emissive power. The material's surface used for this measurement is specular. The incident angle of the measurement was 20 deg. The spectral reflectance of the material changes drastically depending on the temperature. As the material exhibits a metallic state at low temperatures, the IR reflectance indicates higher reflectance spectra than that of 300 K. On the other hand, when the material at high temperatures exhibits a high resistance state, the IR reflectance indicates lower reflectance spectra, with an optical-phonon mode structure, than that of 300 K (Ref. 4). The emissivity was calculated from the following equation,

$$\varepsilon = \frac{\int_0^\infty [1 - R(\lambda)] I_b(\lambda, T)\, d\lambda}{\int_0^\infty I_b(\lambda, T)\, d\lambda} \tag{1}$$

where $R(\lambda)$ is the spectral reflectance and $I_b(\lambda, T)$ is the spectral distribution of the emissive power of a blackbody. As a result, the material shows low emissivity at low temperatures and high emissivity at high temperatures.

Design for Optimum Composition

In the selection of the optimum composition, the requirements for the materials' properties are as follows:

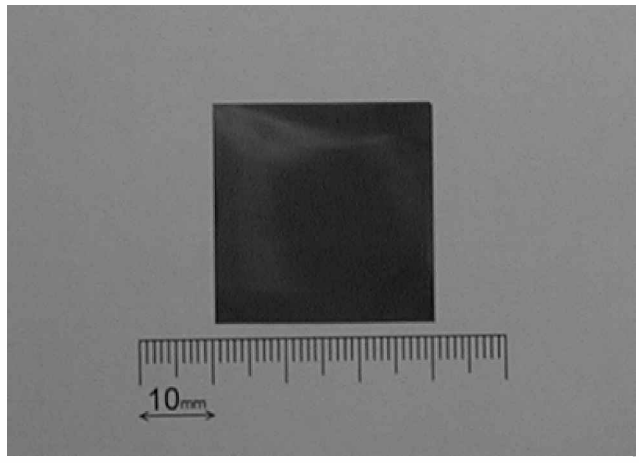

Fig. 2 Test piece of SRD.

1) Because the typical operating temperature range of the constituents on a spacecraft is near room temperature, it is desirable that the transition temperature of the material be at around room temperature.

2) Because ε_{high} influences the area of the SRD and ε_{ratio} influences the amount of heater power used at low temperatures, ε_{high} and ε_{ratio} should be as large as possible.

3) Because the temperature range of the instruments is narrow, the temperature derivative of the emissivity $d\varepsilon/dT$ around transition temperature should be as large as possible to change emissivity dramatically in a narrow temperature range.

The SRD is designed as follows:

1) Some trial SRDs with $La_{1-X}Sr_XMnO_3$ and $La_{1-X}Ca_XMnO_3$ were made, and their optical properties were measured.[5] As a result, the molar ratio X dependence of the total hemispherical emittance became clear.

2) We confirmed that the profile of the temperature dependence of the total hemispherical emittance, such as the transition temperature, is similar to that of the electrical resistivity.[6]

3) From measurement results of the total hemispherical emittance and the electrical resistivity, we selected $La_{0.825}Sr_{0.175}MnO_3$ and $La_{0.7}Ca_{0.3}MnO_3$ as the materials for the SRD.

Preparation of Manganese Oxide

The manganites used for the SRD materials were prepared using standard ceramic techniques as follows[7]:

1) Oxides or carbonates of the metals were weighed in the desired proportions and milled for thorough mixing.

2) The preparations were prefired in air at about 1300 K.

3) The product obtained was milled again, mixed with a binder, and, finally, formed into blocks.

4) The samples were fired over 1300 K again and cut from sintered block.

The sample is a black ceramic tile that is 200 μm thick and weighs only 1.2 kg/m^2. Figure 2 shows a sample of the SRD. The size of the test piece is 30 × 30 mm to simplify manufacturing and measurement. The size of the flight model is 40 × 40 mm.

Optical Properties

Total Hemispherical Emittance

The total hemispherical emittance of the SRD was measured using the calorimetric method.[8] Figure 3 shows the principle of measurement.

The sample is suspended in the center of a chamber by wires for the heater and a thermocouple. When the heater power Q is supplied to the sample, which has area A_S and is equilibrated with total radiant energy from the sample surface to a chamber wall that is cooled to 77 K by LN_2, the total hemispherical emittance ε_H of

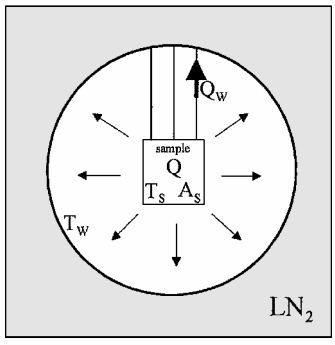

Fig. 3 Principle of measurement.

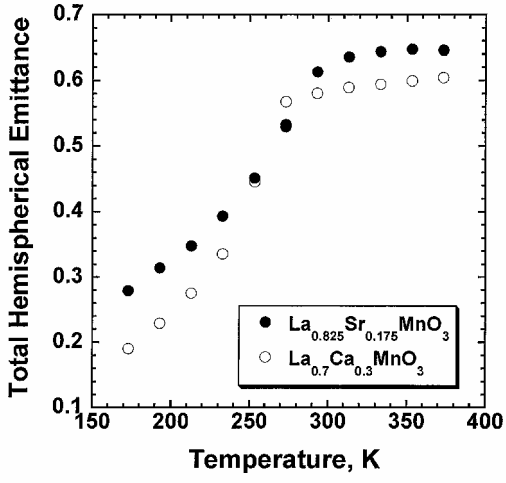

Fig. 4 Temperature dependence of total hemispherical emittance of SRD.

the sample can be expressed as follows:

$$\varepsilon_H(T_S) = \frac{Q - Q_W}{A_S \cdot \sigma \cdot \left(T_S^4 - T_W^4\right)} \tag{2}$$

where Q_W is the heat loss of the sample through thermocouple and wires for the heater, T_S is the equilibrated temperature of the sample, and T_W is the wall temperature of the chamber. The pressure in the chamber is kept under 1.33×10^{-3} Pa using a turbomolecular pump. By measurement of T_S, T_W, and A_S, the total hemispherical emittance ε_H can be obtained. The heat loss Q_W is experimentally measured.[8] The remaining faces of the sample without manganese oxide are covered by metallic aluminum films of known emittance. The main uncertainties in this measurement of ε_H are 1) the temperature of the sample and enclosure walls (±0.54%), 2) the total surface area of the sample (±1.16%), and 3) the ε_H of aluminum thin films (±1.30%). When other small factors are accounted for, the combined standard uncertainty of the total hemispherical emittance measurement was estimated to be at most ±2.2%, from 173.15 to 373.15 K. The reliability of the measured total hemispherical emittance with this system was confirmed by comparing with the calculated total hemispherical emittance using the optical constants, which were measured with the FT–IR in the wavelength range from 2.5 to 100 μm, using aluminum-deposited polyimide films. The measured total hemispherical emittance agreed with the calculations to within 7.0% (Ref. 9).

Figure 4 shows the temperature dependence of the total hemispherical emittance for the SRD. The total hemispherical emittance changes in the temperature range of 173–373 K and, in particular, the emissivity of $La_{0.825}Sr_{0.175}MnO_3$ changes dramatically under 280 K and that of $La_{0.7}Ca_{0.3}MnO_3$ changes dramatically under 260 K. $La_{0.825}Sr_{0.175}MnO_3$ has a high emissivity of 0.65 at high temperatures and a low emissivity of 0.28 at low temperatures, and so the variability of the total hemispherical emittance $\Delta\varepsilon(=\varepsilon_{\text{high}} - \varepsilon_{\text{low}})$ is 0.37 and the ratio of the total hemispherical emittance $\varepsilon_{\text{ratio}}(=\varepsilon_{\text{high}}/\varepsilon_{\text{low}})$ is 2.32. $La_{0.7}Ca_{0.3}MnO_3$ has a high

Table 1 Emissivity of SRD

Material	$\varepsilon_{\text{high}}$	ε_{low}	$\varepsilon_{\text{ratio}}$	$\Delta\varepsilon$
$(La,Sr)MnO_3$	0.65	0.28	2.32	0.37
$(La,Ca)MnO_3$	0.60	0.19	3.16	0.41

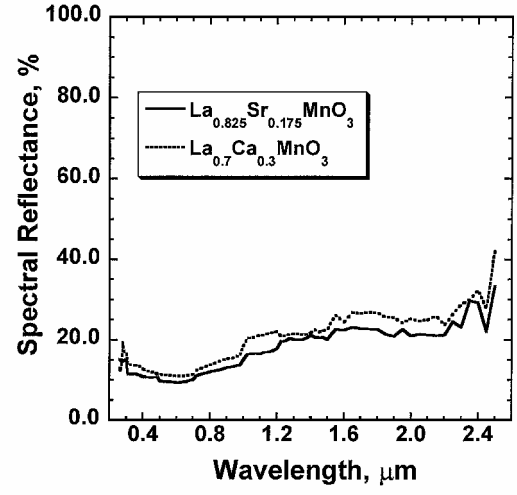

Fig. 5 Spectral reflectance of SRD.

emissivity of 0.60 at high temperatures and a low emissivity of 0.19 at low temperatures, and so the variability $\Delta\varepsilon$ is 0.41 and the ratio $\varepsilon_{\text{ratio}}$ is 3.16. These two materials have different features:

1) $La_{0.825}Sr_{0.175}MnO_3$ has a high T_C and high emissivity at high temperatures.

2) $La_{0.7}Ca_{0.3}MnO_3$ changes its emissivity dramatically at T_C, has low emissivity at low temperatures, and has a large $\varepsilon_{\text{ratio}}$.

Table 1 shows the comparison of the emissivity for two types of the SRD. These two materials have enough variable emissivity to be used as thermal control devices and can be used according to purpose or need, whereas the effective emittance of the thermal louver, for example, changes between 0.1 and 0.8.

The surface of these materials was left unfinished after they were cut, that is, all samples were not polished. In the case of polished samples, the emissivity decreases for all temperatures because there are multiple reflections in the cavities between rough elements when the surface's optical roughness is large, and the roughness increases the trapping of incident radiation. Furthermore, the decrease of emissivity at low temperatures is larger than that at high temperatures, so that the variability of emissivity $\Delta\varepsilon$ and the ratio of emissivity $\varepsilon_{\text{ratio}}$ are larger than those of unpolished samples. The difference of ε_H between unpolished material and polished one is 0.04 at high temperatures and 0.08 at low temperatures.[10] Because the surface condition of the unpolished materials is slightly different, the difference of ε_H of them is less than 0.04 at high temperatures and less than 0.08 at low temperatures.

Solar Absorptance

The solar absorptance was measured spectroscopically with an integrating sphere in the wavelength region of 0.26–2.5 μm, which contains about 96% of the solar radiation intensity. The incidence angle was 5 deg and the sample was at room temperature. Figure 5 shows the experimentally determined reflectivity curves. The solar absorptance was determined by integrating over the solar spectral irradiance curve, as follows:

$$\alpha_S(\theta) = \frac{\int_{0.26}^{2.5}[1 - R(\lambda,\theta)]I_S(\lambda)\,\mathrm{d}\lambda}{\int_{0.26}^{2.5} I_S(\lambda)\,\mathrm{d}\lambda} \tag{3}$$

where $I_S(\lambda)$ is the spectral distribution of solar radiation, $R(\lambda,\theta)$ is the spectral reflectance, and θ is the incident beam angle onto the sample surface. Uncertainties in the measurement are attributed to 1) the value of the spectral reflectance of the reference sample

(±1.0%) and 2) energy loss to the aperture through which light is introduced (±1.0%). The standard uncertainty is estimated to less than ±2.0%. The reliability of the measured solar absorptance was confirmed by comparing with the calculated solar absorptance using the optical constants, similar to the process applied to emittance measurement with the FT–IR. The measured solar absorptance agreed with the calculated value to within 5.0% (Ref. 9).

Both materials show low reflectance. The reflectivity of $La_{0.7}Ca_{0.3}MnO_3$ is a little larger than that of $La_{0.825}Sr_{0.175}MnO_3$ in the wavelength region of 0.26–2.5 μm. The solar absorptance of $La_{0.825}Sr_{0.175}MnO_3$ is 0.87, and that of $La_{0.7}Ca_{0.3}MnO_3$ is 0.84. If the surfaces of the samples were polished, it is expected that the solar absorptance would decrease little. To maximize the benefits to all spacecraft radiating surfaces, a reduction in the solar absorptance is very desirable. To reduce it, a design of multilayer coating that reflects the visible sunlight and acts as an antireflection coating for the thermal IR has previously been applied.[4]

Space Qualification Tests

Radiation durability is required for operation in space because it affects the life of the spacecraft. To evaluate the space degradation of optical properties, space environmental simulation tests were performed on the ground with radiation by protons, electrons, and UV.

Proton Irradiation

The proton irradiation test was performed using a tandem accelerator at the National Institute of Advanced Industrial Science and Technology. Protons were accelerated to energies of 0.5, 1.0, and 2.0 MeV. The exposure rates were 5.0×10^{14} p^+/cm^2, 1.0×10^{13} p^+/cm^2, and 2.0×10^{12} p^+/cm^2, which are equivalent to 10 years at each energy in geostationary orbit. The accuracy of irradiation enrgy is within 1%. The samples were in a vacuum of less than 1.33×10^{-3} Pa, and the sample temperature was kept under 323 K during proton irradiation.

Electron Irradiation

The electron irradiation test was performed using a Cockcroft–Walton accelerator at the Japan Atomic Energy Research Institute. Electrons were accelerated to energies of 0.5, 1.0, and 2.0 MeV. These exposure rates were 1.0×10^{15} e^-/cm^2, 5.0×10^{14} e^-/cm^2, and 2.0×10^{14} e^-/cm^2, which are equivalent to more than 3 years at each energy in geostationary orbit. The irradiation uniformity is less than 3% on the whole area of the sample. The samples were in a vacuum of less than 1.33×10^{-3} Pa, and the sample temperature was kept at less than 323 K during electron irradiation.

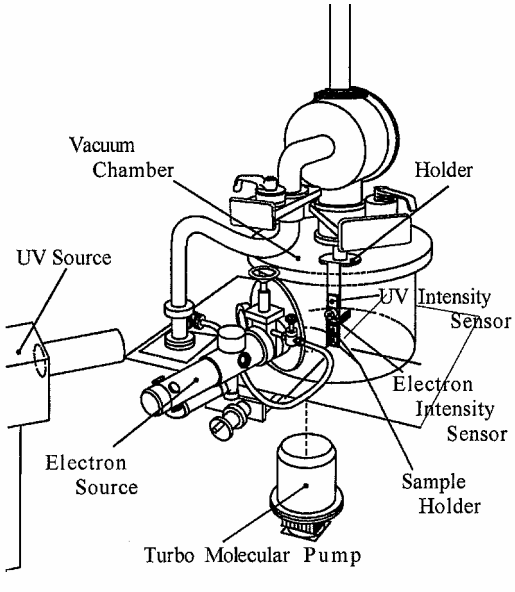

Fig. 6 UV irradiation apparatus.

Table 2 Radiation condition

Energy	Fluence
Protons	
0.5 MeV	5.0×10^{14} p^+/cm^2
1.0 MeV	1.0×10^{13} p^+/cm^2
2.0 MeV	2.0×10^{12} p^+/cm^2
Electrons	
0.5 MeV	1.0×10^{15} e^-/cm^2
1.0 MeV	5.0×10^{14} e^-/cm^2
2.0 MeV	2.0×10^{14} e^-/cm^2
UV	
11.5 SC	11532.8 ESH

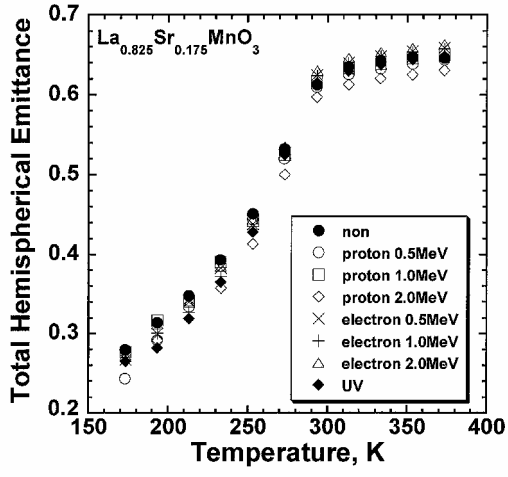

Fig. 7 Effects of protons, electrons, and UV irradiation on total hemispherical emittance of $La_{0.825}Sr_{0.175}MnO_3$.

UV Irradiation

The UV irradiator source is a 2-kW Hg–Xe short arc lamp. Its intensity can be changed from 0.2 to 14.0 times the solar constant (SC) in the wavelength region from 0.2 to 0.5 μm. The UV source intensity is uniform within 10% all over the sample surface. The samples were in a vacuum of less than 1.33×10^{-3} Pa, attained by a turbomolecular pump. The temperature of these samples was kept at less than 353 K. The intensity was set at about 11.5 SC in the test to accelerate the degradation. The total exposure time was 11,532.8 equivalent sun hours (ESH), where ESH is equal to a product of exposure time and exposure illuminant. Figure 6 shows the apparatus for UV irradiation.

Table 2 gives the overview for the test conditions of protons, electrons, and UV irradiation. The irradiated samples were stored in a vacuum and in the dark.

Experimental Results

To investigate the effect of degradation for proton, electron, and UV irradiation, the total hemispherical emittance and the solar absorptance were measured before and after irradiation. These samples used in the irradiation tests showed no visible degradation or external damage as a result of these tests.

Total Hemispherical Emittance

Figures 7 and 8 shows the temperature dependence of the total hemispherical emittance for $La_{0.825}Sr_{0.175}MnO_3$ and $La_{0.7}Ca_{0.3}MnO_3$ before and after irradiation. The ε_H shows almost the same behavior in the entire temperature range, and there are no notable differences between samples. The property that the ε_H changes dramatically is not affected by irradiation.

Solar Absorptance

The solar absorptance was measured before and after irradiation. Table 3 shows the variation of the solar absorptance $\Delta\alpha_S (= \alpha_{S,\text{after}} - \alpha_{S,\text{before}})$. The variation between samples is less

Table 3 Effect of protons, electrons, and UV irradiation on solar absorptance of SRD

Source	$\Delta\alpha_S$
(La,Sr)MnO_3, proton	
0.5 MeV	0.00
1.0 MeV	0.00
2.0 MeV	0.00
(La,Sr)MnO_3, electron	
0.5 MeV	−0.01
1.0 MeV	0.00
2.0 MeV	0.00
UV	
——	0.00
(La,Ca)MnO_3, proton	
0.5 MeV	0.00
1.0 MeV	0.00
2.0 MeV	0.00
(La,Ca)MnO_3, electron	
0.5 MeV	−0.01
1.0 MeV	0.00
2.0 MeV	0.00
UV	
——	0.00

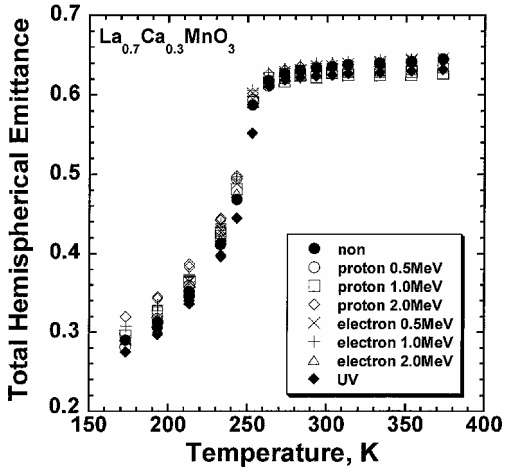

Fig. 8 Effects of protons, electrons, and UV irradiation on total hemispherical emittance of $La_{0.7}Ca_{0.3}MnO_3$.

than 0.01. Therefore, no degradation was observed in optical properties for the samples we measured.

From these results, we confirmed that there was no degradation of $La_{0.825}Sr_{0.175}MnO_3$ and $La_{0.7}Ca_{0.3}MnO_3$ for proton, electron, and UV irradiation.

Summary

Two thermal control materials using manganese oxides with a perovskite structure have been developed. The materials are a variable emittance radiator called an SRD. The temperature dependence of the total hemispherical emittance and the solar absorptance around room temperature have been measured. The effects for proton, electron, and UV irradiation on optical properties have been investigated. The major features of the SRD can be summarized as follows:

1) The SRD changes its emissivity according to its own temperature, without electrical instruments or mechanical parts.

2) The material is a thin and light ceramic tile that is easy to attach to the external surface of a spacecraft.

3) There is no degradation of the optical properties of the materials by proton, electron, and UV irradiation.

4) The solar absorptance of the materials are so high that it is necessary to cover the materials with a mirror composed of a infrared transparent material in cases where the SRD is used on a surface that is facing the sun.

The heater power, mass, and cost savings that can be realized with the SRD are potentially significant for many future spacecraft design applications. In addition, the SRD allows a more flexible thermal design, which is especially important for spacecraft for which the orbit parameters are not well defined or known during the design period.

The SRD will be used in the scientific satellite MUSES-C of the Institute of Space and Astronautical Science, which is going to perform a sample return mission to a near-Earth asteroid. After that, the thin-film SRD will be tested by the flight of INDEX, which is a small engineering satellite that will be exposed to all kinds of degrading environmental loads. These missions will demonstrate SRD technologies and provide validation for their use in future spacecraft.

Acknowledgments

The authors thank Y. Morita for cooperation in the irradiation test of electrons and A. Chayahara for cooperation in the irradiation test of protons.

References

[1]Gilmore, D. G., "Chapter IV—Thermal Control Hardware," *Satellite Thermal Control Handbook*, The Aerospace Corp. Press, EL Segundo, CA, 1994, pp. 4-99–4-121.

[2]Okimoto, Y., Katsufuji, T., Ishikawa, T., Arima, T., and Tokura, Y., "Variation of Electronic Structure in $La_{1-X}Sr_XMnO_3$ ($0 \leq X \leq 3$) as Investigated by Optical Conductivity Spectra," *Physical Review B*, Vol. 55, No. 7, 1997, pp. 4206–4214.

[3]Zener, C., "Interaction Between the d-Shells in the Transition Metals. II. Ferromagnetic Compounds of Manganese with Perovskite Structure," *Physical Review*, Vol. 82, No. 3, 1951, pp. 403–405.

[4]Shimazaki, K., Tachikawa, S., Ohnishi, A., and Nagasaka, Y., "Design of Thermal Radiative Properties of Multilayer Films on a Variable Emittance Radiator," The Engineering Society for Advancing Mobility Land Sea Air and Space, Paper 2001-01-2339, July 2001.

[5]Shimazaki, K., Tachikawa, S., Ohnishi, A., and Nagasaka, Y., "Design and Preliminary Test Results of Variable Emittance Device," *Proceedings of 8th International Symposium on Materials in Space Environment*, Centre National D'Etudes Spatiales, Toulouse, France, 2000.

[6]Urushibara, A., Moritomo, Y., Arima, T., Kido, G., and Tokura, Y., "Insulator–Metal Transition and Giant Magnetoresistance in $La_{1-X}Sr_XMnO_3$," *Physical Review B*, Vol. 51, No. 20, 1995, pp. 14103–14109.

[7]Jonker, G. H., and Van Santen, J. H., "Feromagnetic Compounds of Manganese with Perovskite Structure," *Physica*, Vol. 16, No. 3, 1950, pp. 337–349.

[8]Ohnishi, A., Hayashi, T., and Nagano, H., "Measurement of Hemispherical Total Emittance of Thermal Control Materials for Spacecraft," *Proceedings of 4th Japan Symposium on Thermophysical Properties*, Japan Society of Thermophysical Properties, Kyushu Univ., Kasuga, Japan, 1983, pp. 1–4.

[9]Horikoshi, R., Nagasaka, Y., and Ohnishi, A., "A Method of Calculating Thermal Radiation Properties of Multilayrer Films from Optical Constans," *International Journal of Thermophysics*, Vol. 19, No. 2, 1998, pp. 547–555.

[10]Shimazaki, K., Tachikawa, S., Ohnishi, A., and Nagasaka, Y., "Temperature Dependence of Total Hemispherical Emittance in Perovskite-Type Manganese Oxides, $La_{1-X}Sr_XMnO_3$," *High Temperatures–High Pressures*, 2001, Vol. 33, pp. 525–531.